Progressive Decline in the Ability of Calmodulin Isolated from Aged Brain To Activate the Plasma Membrane Ca-ATPase†

Jun Gao,‡ Dan Yin,‡ Yihong Yao,‡ Todd D. Williams,§ and Thomas C. Squier*,‡

Department of Biochemistry, Cell & Molecular Biology, and Mass Spectrometry Laboratory, University of Kansas, Lawrence, Kansas 66045-2106

Received February 18, 1998; Revised Manuscript Received April 27, 1998

ABSTRACT: To identify possible relationships between the loss of calcium homeostasis in brain associated with aging and alterations in the function of key calcium regulatory proteins, we have purified calmodulin (CaM) from the brains of Fischer 344 rats of different ages and have assessed age-related alterations in (i) the secondary and tertiary structure of CaM and (ii) the ability of CaM to activate one of its target proteins, the plasma membrane (PM) Ca-ATPase. There is a progressive, age-dependent reduction in the ability of CaM to activate the PM-Ca-ATPase, which correlates with the oxidative modification of multiple methionines to their corresponding methionine sulfoxides. No other detectable age-related posttranslational modifications occur in the primary sequence of CaM, suggesting that the reduced ability of CaM to activate the PM-Ca-ATPase is the result of methionine oxidation. Corresponding age-related changes in the secondary and tertiary structure of CaM occur, resulting in alterations in the relative mobility of CaM on polyacrylamide gels, differences in the intrinsic fluorescence intensity and solvent accessibility of Tyr_{99} and Tyr_{138}, and a reduction in the average α-helical content of CaM at 20 °C. Shifts in the calcium- and CaM-dependent activation of the PM-Ca-ATPase are observed for CaM isolated from senescent brain, which respectively requires larger concentrations of either calcium or CaM to activate the PM-Ca-ATPase. The observation that the oxidative modification of CaM during normal biological aging results in a reduced calcium sensitivity of the PM-Ca-ATPase, a lower affinity between CaM and the PM-Ca-ATPase, and the reduction in the maximal velocity of the PM-Ca-ATPase is consistent with earlier results that indicate the calcium handling capacity of a range of tissues including brain, heart, and erythrocytes isolated from aged animals declines, resulting in both longer calcium transients and elevated basal levels of intracellular calcium. Thus, the oxidative modification of selected methionines in CaM may explain aspects of the loss of calcium homeostasis associated with the aging process.

Oxidatively modified proteins accumulate during aging and have been suggested to contribute to the loss of cellular function associated with a host of age-related diseases, including amyotrophic lateral sclerosis, Alzheimer's disease, muscular dystrophy, atherosclerosis, diabetes, and Parkinson's disease (*1*, *2*). However, while all amino acids can be oxidatively modified, cysteine and methionine residues are particularly sensitive to modification by most reactive oxygen species (ROS)[1] and are the only amino acids that can be repaired by endogenous reductases present in all cells (*3*). These latter modifications therefore have the potential to regulate intracellular signaling and could function as endogenous antioxidant systems that may protect other essential residues within proteins from irreversible oxidative modification (*4*, *5*). Consistent with a possible regulatory role involving methionine oxidation, the functional ability of the calcium signaling protein calmodulin (CaM) to activate a range of target proteins, including the plasma membrane (PM) Ca-ATPase, is inhibited upon methionine oxidation (*6*−*10*). Since oxidatively modified CaM (CaM_{ox}) binds to the PM-Ca-ATPase and prevents its activation by native (unoxidized) CaM, the reversible oxidative modification of CaM provides a possible mechanism to modulate ATP utilization and enhance the probability of cellular survival under conditions of oxidative stress (*4*, *9*). Furthermore, since CaM functions to modulate intracellular calcium homeostasis

† This work was supported by the National Institutes of Health (Grant AG12993). The tandem mass spectrometer and electrospray source were respectively obtained through grants from the National Institutes of Health (S10 RR0 6294) and the National Science Foundation (CHE-9413975).

* Correspondence should be addressed to this author. Tel, 785-864-4008; fax, 785-864-5321; e-mail, TCSQUIER@KUHUB.CC.UKANS.EDU.

‡ Department of Biochemistry, Cell & Molecular Biology.

§ Mass Spectrometry Laboratory.

[1] Abbreviations: CaM, calmodulin; CaM_{ox}, oxidatively modified calmodulin; CaM oxiform, a population of CaM species containing a specific integral number of incorporated oxygens; H_2O_2, hydrogen peroxide; CD, circular dichroism; CID, collision-induced dissociation; DTT, dithiothreitol; EDTA, ethylenediaminetetraacetic acid; EGTA, ethylene glycol bis(β-aminoethyl ether)-*N*,*N*,*N*′,*N*′-tetraacetic acid; ESI-MS, electrospray ionization mass spectrometry; FAB-MS, fast atom bombardment mass spectrometry; FURA-2, 1-[2-(5-carboxylazol-2-yl)-6-aminobenzofuran-5-oxyl]-2-(2-amino-5-methylphenoxy)ethane-*N*,*N*,*N*,*N*-tetracetic acid; HEPES, *N*-(2- hydroxyethyl)piperazine-*N*′-2-ethansulfonic acid; HPLC, high performance liquid chromatography; Met, methionine; Met(O), methionine sulfoxide; MS, mass spectrometry; PM, plasma membrane; ROS, reactive oxygen species; SDS−PAGE, sodium dodecyl sulfate−polyacrylamide gel electrophoresis; TEMPAMINE, 4-amino-2,2,6,6-tetramethyl-1-piperidinyloxyl; TFA, trifluoroacetic acid.

S0006-2960(98)00387-0 CCC: $15.00
Published on Web 06/11/1998

through the feed-forward activation of the PM-Ca-ATPase and the feedback inhibition of the ryanodine receptor (*11*, *12*), it is possible that age-related alterations in the functional properties of CaM may explain, in part, the age-related decline in calcium handling capabilities in excitable cells (*13*, *14*).

To identify posttranslational modifications in CaM that may explain aspects of the age-related decline in calcium regulation observed in cells isolated from aged organisms, we have investigated the function and structure of CaM isolated from the brains of Fischer 344 rats ranging in age from 6 to 26 months. We report an age-related decline in the ability of CaM to activate the PM-Ca-ATPase that correlates with the oxidative modification of multiple methionines to their corresponding sulfoxides. Accompanying these posttranslational modifications within the primary sequence of CaM are global structural changes that diminish the calcium-dependent conformational coupling between the high affinity calcium binding sites in CaM that normally functions in the mechanism of calcium activation. These latter results are consistent with the proposal that the oxidative modification of CaM during aging may compromise intracellular calcium regulation. A preliminary account of this work was presented at a symposium regarding "The Current Status of the Calcium Hypothesis of Brain Aging and Alzheimer's Disease" at Internationales Wissenschaftsforum der Universität Heidelberg (*15*).

EXPERIMENTAL PROCEDURES

Materials. All reagent chemicals were the purest grade commercially available. $^{45}CaCl_2$ was obtained from ICN (Costa Mesa, CA); type XIII TPCK-treated trypsin and type I-S soybean trypsin inhibitor were from VWR Scientific (Baltimore, MD). Prestained molecular weight markers were purchased from Bio-Rad Laboratories (Richmond, CA). 1-[2-(5-Carboxylazol-2-yl)-6-aminobenzofuran-5-oxyl]-2-(2-amino-5-methylphenoxy)ethane-*N*,*N*,*N*′,*N*′-tetraacetic acid) (FURA-2) was obtained from Molecular Probes, Inc. (Juntion City, OR). CaMKII20 (LKKPNARRKLKGAILTTMLA), the CaM binding sequence in CaM-dependent protein kinase IIα, was purchased from Signal Transduction Inc. (San Diego, CA). C28W (LRRGQILWFRGLNRIQTQIRVVNAFRSS), a peptide identical to the CaM binding sequence of the PM-Ca-ATPase, was synthesized by Quality Controlled Biochemicals, Inc. (Boston, MA). Rabbit monoclonal anti-calmodulin antibody was purchased from STI (San Diego, CA). Secondary goat anti-mouse antibodies conjugated to alkaline phosphatase were obtained from Sigma (St. Louis, MO). Erythrocyte ghost plasma membranes were purified from porcine blood, as previously described (*16*). CaM was isolated from the brains of Fischer 344 strain male rats aged 5, 10, 6, and 26 months (see below), which were obtained from the National Institute of Aging maintained rat colony (Harlan Sprague Dawley, Indianapolis). Purified CaM and erythrocyte ghost membranes were stored at −70 °C.

CaM Purification. Rat brain CaM was purified essentially as described by Strasburg and co-workers (*17*), with the following two modifications: (i) β-mercaptoethanol or DTT was not included in any procedure to avoid potential reduction of oxidized CaM, and (ii) all buffers were saturated with argon during the entire procedure to avoid possible oxidative modifications in CaM. The CaM concentration was determined using the Micro BCA assay (Pierce, Rockford, IL), using salt-free bovine brain CaM as a standard. The concentration of the CaM standard was determined using the published molar extinction coefficient ($\epsilon_{277} = 3029\ M^{-1}\ cm^{-1}$) for the calcium-saturated enzyme (*17*, *18*). CaM was estimated to be greater than 99% pure as assessed by SDS−PAGE and HPLC.

Enzymatic Assays. The ATPase activity of the erythrocyte ghost PM-Ca-ATPase (0.2 mg mL^{-1} porcine erythrocyte ghost membranes) was measured at 37 °C in 50 mM MOPS (pH 7.0), 0.1 M KCl, 5 mM $MgCl_2$, 5 mM ATP, 100 μM EGTA, and 4 μM A23187 in the presence of variable amounts of calcium or CaM (see below) using the method described by Lanzetta and co-workers (*19*) for measuring the release of phosphate. The CaM-dependent activation of the PM-Ca-ATPase was measured in the presence of 0.1 mM $CaCl_2$ to saturate the calcium binding sites of both CaM and the PM-Ca-ATPase fully. The calcium-dependent activation of the PM-Ca-ATPase was measured in the presence of 0.3 μM CaM to fully saturate all CaM-binding sites on the erythrocyte Ca-ATPase, and the free calcium concentration was measured using FURA-2 ($\lambda_{ex} = 340$ nm; $\lambda_{em} = 510$ nm), as described previously (*20*). The ghost membrane protein concentration was determined by the method of Biuret (*21*), using BSA as the standard. The amount of CaM in total brain homogenates was determined with antibodies directed against CaM using an enzyme-linked immunosorbent (ELISA) assay, essentially as previously described (*22*).

Quantification of Protein Carbonyls. Total carbonyl content in CaM involved the measurement of a DNPH adduct with CaM using the published molar extinction coefficient ($\epsilon_{370} = 2.2 \times 10^4\ M^{-1}\ cm^{-1}$), as described in detail elsewhere (*23*).

Polyacrylamide Gel Electrophoresis. Native and sodium dodecyl sulfate−polyacrylamide gel electrophoresis (SDS−PAGE) were done as previously described (*24*, *25*). To detect calcium-dependent structural changes, either 0.1 mM $CaCl_2$ or 0.1 mM EGTA was added to the sample buffer, running buffer, and gel buffers. Protein bands were visualized with 0.04% Coomassie blue G in 3.5% perchloric acid for 2 h. The destaining solution contains 5% methanol and 7.5% acetic acid.

Proteolytic Digestion. The exhaustive tryptic digestion of CaM involved the addition of 0.6 μM trypsin to 60 μM CaM in 50 mM potassium phosphate (pH 8.0) for 9 h at 37 °C. Digestion was stopped by the addition of 1.8 μM trypsin inhibitor.

Equilibrium Dialysis. The stoichiometry of calcium binding to CaM was determined using 0.2 mM $^{45}CaCl_2$ (10 000 cpm/nmol) equilibrated with 30 μM CaM (0.5 mg/mL) using a 1-mL dialysis cell separated by a dialysis membrane with a molecular weight cutoff less of 10 000 Da in a buffer containing 100 mM HEPES (pH 7.5), 0.1 M KCl, and 1 mM $MgCl_2$, essentially as previously described (*26*).

Reversed-Phase HPLC. After exhaustive tryptic digestion of CaM, individual proteolytic fragments were separated using a Vydac C4 reversed-phase column employing a linear gradient of acetonitrile that varied from 0% acetonitrile in 0.1% TFA to 90% acetonitrile in 0.1% TFA at a rate of 1%/min, as previously described (*9*). The respective peaks were monitored at 214 nm. To identify the proteolytic fragments,

the detected peaks were pooled, lyophilized, and subjected to fast atom bombardment (FAB) mass spectrometry (see below).

Fluorescence Spectroscopy Measurements. Steady-state fluorescence intensities were measured using a Fluoro Max-2 (Jobin Yvon Spex, Edison, NJ) equipped with a xenon lamp. Excitation was at 275 nm for tyrosine and at 298 nm for tryptophan. Measurements of calcium-dependent alterations in the solvent accessibility of Tyr_{99} and Tyr_{138} involved the addition of the water-soluble quencher TEMPAMINE, and the Stern−Volmer quenching constant (K_{sv}) was determined as previously described (*27*).

Mass Spectrometry. The distributions of CaM oxiforms were measured using an AUTOSPEC-Q instrument equipped with the Mark III ESI source, essentially as previously described (*28*). FAB-MS spectra were obtained on an AUTOSPEC-Q tandem hybrid mass spectrometer using a cesium gun operated at 20 keV energy and 2 μA emission, as described previously (*9*). Mass identification was assisted by software (GPMAW from lighthouse data, Aalokken 14, DK-5250, Odense SV, Denmark) that permits the identification of each tryptic fragment.

Circular Dichroism Spectroscopy. Spectra of salt-free CaM (50 μg/mL) in 10 mM Tris-HCl (pH 7.5), 0.1 M $KClO_4$, 1 mM $Mg(ClO_4)_2$, and 0.1 mM $Ca(ClO_4)_2$ were measured using a Jasco J-710 spectropolarimeter using a temperature jacketed spectral cell with a path length of 0.5 cm. CD spectra were collected between 200 and 240 nm, and the α-helical content was estimated using the computer program Contin (*29*). In all cases, the experimental errors associated with the experimental determination of the α-helical content of CaM were approximately 1%.

Calculation of Model-Dependent Fitting Parameters. To explicitly analyze for the relative affinities and cooperative interactions between the individual ligand binding sites, data was fit to

$$Y = \frac{K_1[\mathrm{X}]_{\mathrm{free}} + 2K_2[\mathrm{X}]_{\mathrm{free}}^{\ 2}}{2(1 + K_1\,[\mathrm{X}]_{\mathrm{free}} + K_2[\mathrm{X}]_{\mathrm{free}}^{\ 2})} \quad (1)$$

where X corresponds to the concentration of ligand (i.e., calcium or CaM), K_1 is the macroscopic equilibrium constant that corresponds to the sum of the intrinsic equilibrium constants (k_1 and k_2) associated with ligand binding to the two classes of binding sites, and K_2 represents the intrinsic equilibrium constant for binding ligand to both classes of ligand binding sites ($k_1k_2k_c$), where k_c provides a quantitative estimate of the lower limit with respect to the cooperative interactions between the sites (*30*).

An analogous expression useful with respect to the analysis of CaM binding to target peptides is the equivalent Scatchard form of the binding equation (*31*):

$$[\mathrm{CaM}]_{\mathrm{bound}} = \left[\frac{(K_2[\mathrm{CaM}]_{\mathrm{free}} + 1)(K_1[\mathrm{CaM}]_{\mathrm{free}})}{1 + (K_1[\mathrm{CaM}]_{\mathrm{free}}) + (K_1K_2[\mathrm{CaM}]_{\mathrm{free}}^{\ 2})}\right] \times \text{maximal binding} \quad (2)$$

Since one CaM binds to C28W (*32*, *33*), K_1 and K_2 represent the association constants for each domain on CaM with respect to its association with the target peptide. Binding curves were measured using the CaM-dependent changes in fluorescence intensity associated with Trp_4 on the target peptide C28W, as previously described (*9*). In all cases, data were fit using the Levenberg−Marquardt algorithm contained in the programs ORIGIN (Microcal Software, Inc., Northampton, MA) and Mathcad (MathSoft Inc., Cambridge, MA) to extract free energy parameters relating to the properties of the native and oxidatively modified CaM (*34*).

Calculation of Age-Dependent Alterations in CaM Stability. Alterations in the free energy associated with the stability of CaM were analyzed using a simple two-state model that assumes a highly cooperative temperature-dependent denaturation of the α-helical content of CaM (*35*), where

$$\Delta\Delta G'_{T_m} = \Delta G'_{\mathrm{aged}} - \Delta G'_{\mathrm{young}} = -RT_m \ln \frac{[\alpha\text{-helix}_{\mathrm{aged}}]_{T_m}}{[\alpha\text{-helix}_{\mathrm{aged}}]_{10\ ^\circ\mathrm{C}} - [\alpha\text{-helix}_{\mathrm{aged}}]_{T_m}} \quad (3)$$

$\Delta\Delta G'$ is the increase in free energy for CaM isolated from senescent (26 month) brains relative to that of young (6 month) CaM in kcal mol^{-1}, T_m is the temperature in K where the α-helical content of CaM isolated from young brain is 50% of that at 10 °C, and R is the gas constant.

RESULTS

Abundance of CaM. To identify possible age-related alterations in either the expression levels or the function of CaM, we have isolated CaM from the brains of Fischer 344 rats of varying ages. The amount of immunoreactive CaM present in the homogenates of brains was measured using monoclonal antibodies directed against CaM using an ELISA assay. Immunoreactive CaM obtained from 26 month animals (1.4 ± 0.2 mg/g of brain) is less than that observed for CaM isolated from younger animals that were either 6 (1.8 ± 0.1 mg/g of brain) or 16 month (2.0 ± 0.4 mg/g of brain) of age ($p < 0.05$). Using affinity chromatography to purify CaM, we recover 32 ± 6% and 39 ± 7% of the total CaM present in the crude homogenate obtained from young and senescent brain. These similar purification efficiencies suggest that any significant population of CaM that is structurally modified with age is retained throughout the purification procedure.

CaM-Dependent Activation of the PM-Ca-ATPase. In comparison to the CaM-dependent activation of the PM-Ca-ATPase observed using CaM isolated from young (6 month) animals, there is a 21 ± 2% reduction in the maximal activation (V_{max}) of the PM-Ca-ATPase for CaM isolated from senescent (26 month) animals (Figure 1). This age-dependent decrease in the maximal activation of the PM-Ca-ATPase by CaM is progressive (Figure 1C). Thus, age-related modifications with respect to the ability of CaM to activate the PM-Ca-ATPases are probably a manifestation of the aging process per se, and are not the result of pathological alterations in metabolism that may accompany the end stage of the aging process (*36*).

In the presence of saturating concentrations of CaM, there is a shift in the calcium-dependent activation of the PM-Ca-ATPase toward higher calcium concentrations for CaM isolated from senescent (26 month; $[Ca]_{1/2} = 0.97 \pm 0.07$ μM) animals relative to that observed for CaM isolated from

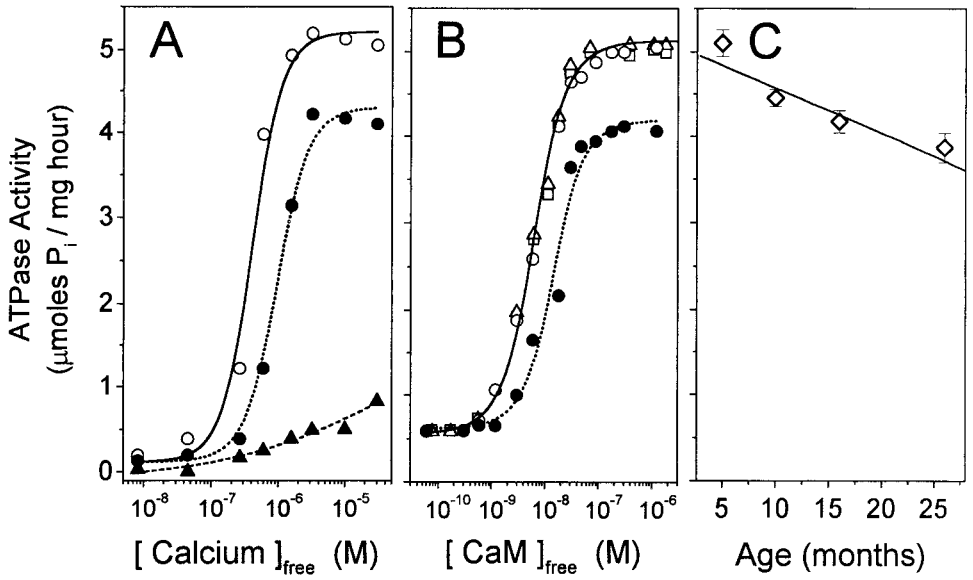

FIGURE 1: Decreased activation of the PM-Ca-ATPase by CaM isolated from aged brain. ATPase activity of porcine erythrocyte ghost plasma membrane Ca-ATPase was measured in the absence (▲) and the presence of CaM isolated from the brains of 6 (○) and 26 month (●) Fischer 344 rats in the presence of either 0.3 μM CaM (A) or 30 μM free calcium (B). For comparison, the CaM-dependent activation of the PM-Ca-ATPase by CaM isolated from bovine testes (□) or wheat germ (△) is shown. The maximal activation (V_{max}) of the PM-Ca-ATPase by CaM isolated from brains of variable age is shown in panel C (◇). ATPase activity was measured at 37 °C in a reaction mixture containing 0.2 mg mL^{-1} erythrocyte ghost membrane protein (approximately 8 nM Ca-ATPase), 0.1 M KCl, 5 mM $MgCl_2$, 100 μM EGTA, 50 mM MOPS (pH 7.0), 5 mM ATP, and 4 μM A23187; phosphate release was measured as previously described (*19*). Free CaM concentrations were calculated by correcting for CaM bound to the PM-Ca-ATPase (40 pmol of CaM/mg of ghost protein), as previously described (*9*). Experimental data shown in panels A and B represent the average values obtained from two measurements, where the standard deviation in the ATPase measurement is 5% of the indicated values. Panel C shows the average CaM-dependent activation and associated standard errors of the mean observed for four different preparations (3 brains per preparation). Experimental curves in panels A and B were obtained from a least-squares fit to eq 1. For panel A: ΔG_1 (6 month) = -7.2 ± 0.5 kcal mol^{-1}, ΔG_2 (6 month) = -17.4 ± 0.1 kcal mol^{-1}, and ΔG_c (6 month) = -3.8 ± 0.5 kcal mol^{-1}. ΔG_1 (26 month) = -7.2 ± 0.5 kcal mol^{-1}, ΔG_2 (26 month) = -16.5 ± 0.1 kcal mol^{-1}, and ΔG_c (26 month) = -2.8 ± 0.5 kcal mol^{-1}. For panel B, ΔG_1 (6 month) = -9.3 ± 0.5 kcal mol^{-1}, ΔG_2 (6 month) = -20.6 ± 0.1 kcal mol^{-1}, and ΔG_c (6 month) = -1.0 ± 0.2 kcal mol^{-1}. ΔG_1 (26 month) = -9.9 ± 0.5 kcal mol^{-1}, ΔG_2 (26 month) = -20.0 ± 0.1 kcal mol^{-1}, and ΔG_c (26 month) = -0.3 ± 0.2 kcal mol^{-1}.

young (6 month; $[Ca]_{1/2} = 0.42 \pm 0.01$ μM) animals (Figure 1A). These latter results suggest that CaM isolated from senescent animals has a reduced calcium affinity or that cooperative interactions between the high affinity calcium binding sites are diminished. To further characterize the age-related alterations in the ability of CaM to activate the PM-Ca-ATPase, we investigated the CaM-dependent activation of the PM-Ca-ATPase in the presence of saturating calcium concentrations. CaM isolated from 6 month Fischer 344 rat brains has a similar ability to activate the PM-Ca-ATPase relative to that obtained using CaM isolated from either bovine testes or wheat germ (Figure 1B). In contrast, independent of the CaM concentration, the maximal activation of the PM-Ca-ATPase by CaM isolated from senescent brain is less than that obtained using CaM isolated from young brain. Furthermore, there is a shift in the concentration dependence of the CaM-dependent activation of the PM-Ca-ATPase using CaM obtained from senescent individuals toward a higher CaM concentration ($[CaM]_{1/2} = 14 \pm 2$ nM) relative to that observed using CaM isolated from young brain ($[CaM]_{1/2} = 6.4 \pm 0.3$ nM). The inability to recover the full activation of the PM-Ca-ATPase by increasing the concentration of CaM isolated from senescent brain indicates that all binding sites on the PM-Ca-ATPase are saturated, and suggests that a subpopulation of CaM species isolated from senescent brains binds but is unable to fully activate the PM-Ca-ATPase. These latter results suggest that alterations to CaM in aged cells can have a major impact on intracellular signaling and metabolism through their ability to block normal regulation of critical intracellular targets (e.g., PM-Ca-ATPase).

Resolution of CaM Heterogeneity Using SDS−PAGE. We have used SDS−PAGE to identify possible age-related alterations in the structure of CaM. CaM isolated from the brains of young (6 month) animals migrates with an apparent molecular mass of about 12 kDa (Figure 2A), and the average apparent molecular mass increases in a progressive manner for CaM isolated from the brains of Fischer 344 rats whose age varies from 10 ($M_r \approx 13$ kDa), 16 ($M_r \approx 15$ kDa), to 26 months ($M_r \approx 18$ kDa). Furthermore, while CaM isolated from young (6 month) animals migrates as a narrow band, considerable heterogeneity appears in CaM isolated from 10 and 16 month animals. CaM isolated from the 26 month animals once again exhibits a narrow band similar to that of CaM isolated from 6 month animals, indicating that CaM isolated from these older animals exhibits less structural heterogeneity. These alterations in gel mobility cannot be explained as the result of age-related differences in the expression of different CaM isoforms, since there is only a single isoform of CaM expressed in all vertebrates (*37*). Thus, changes in either posttranslational modifications in the primary sequence or in the tertiary structure of CaM alter its mobility on SDS polyacrylamide gels.

Calcium-Dependent Alterations in the Mobility of CaM on Polyacrylamide Gels. CaM retains considerable structure in SDS, and calcium-dependent changes in the mobility of CaM on SDS−PAGE have been routinely used to assess structural changes associated with calcium activation (*9*, *38*,

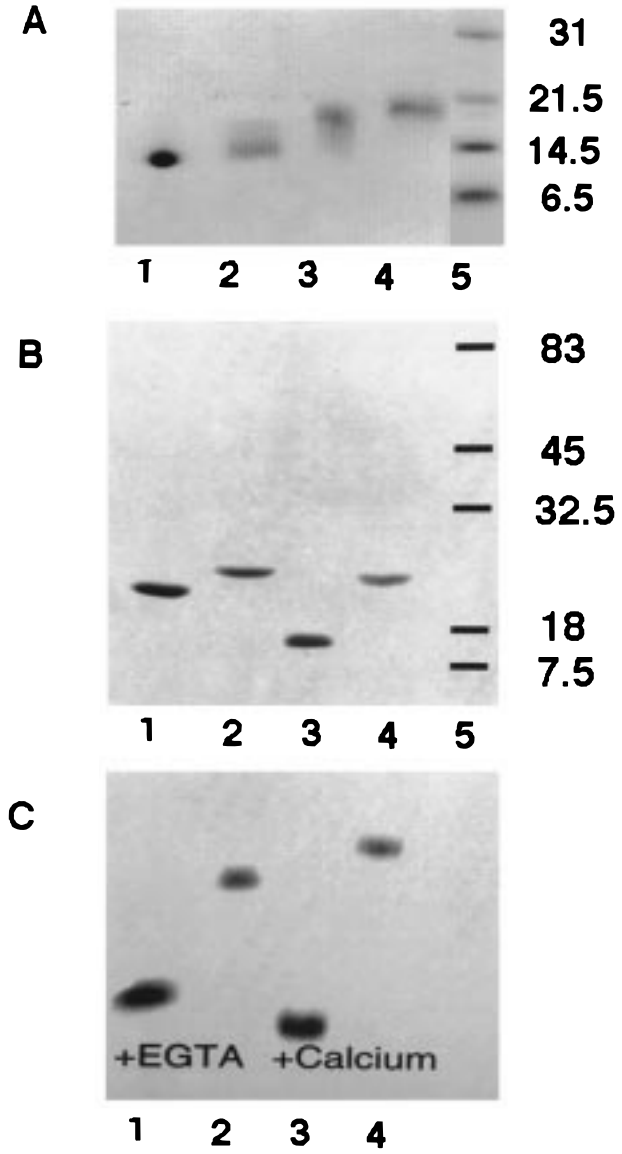

FIGURE 2: Electrophoretic mobility of CaM isolated from aged brain. A comparison of the mobility of CaM isolated from the brains of 6 (lane 1), 10 (lane 2), 16 (lane 3), and 26 month (lane 4) Fischer 344 rats was visualized using a 7−17% acrylamide gradient gel using SDS−PAGE (A). Calcium-dependent shifts in electrophoretic mobility for CaM isolated from 6 (lanes 1 and 3) and 26 month (lanes 2 and 4) rat brains were visualized using both SDS− PAGE (B) and native gels (C) using either a 7−17% acrylamide gradient or a 10% acrylamide gel. SDS−PAGE and native gel electrophoresis were performed as previously described (*24*, *25*). Sample conditions included 0.6 nmol of CaM with either 1 mM $CaCl_2$ (+calcium; lanes 3 and 4) or 1 mM EGTA (+EGTA; lanes 1 and 2) in both sample and running buffers. Molecular mass standards (lane 5) correspond to either Coomassie brilliant blue stained standards (A) or prestained kaleidoscope molecular mass standards (B) and represent aprotinin (6.5 and 7.5 kDa, respectively), lysozyme (14.5 and 18 kDa, respectively), trypsin inhibitor (21.5 and 32.6 kDa, respectively), and carbonic anhydrase (31 and 45 kDa, respectively). Differences in the molecular masses of these protein standards are the result of the derivitization of these proteins in the kaleidoscope molecular mass standards. Protein bands were visualized using Coomassie brilliant blue.

39). The narrow distribution of molecular species apparent in CaM isolated from the brains of either young (6 month) or senescent (26 month) animals (see above) permit the use of these gel mobility assays (Figure 2B). The presence of calcium alters the apparent molecular mass of CaM on SDS−PAGE isolated from the brains of young rats from approximately 17 ± 1 to 12 ± 1 kDa. In contrast, CaM isolated from the brains of senescent rats exhibits a loss of this calcium-induced change in mobility; the apparent molecular mass of CaM is 19 ± 1 to 18 ± 1 kDa in the absence and the presence of calcium, respectively (Figure 2B). These results indicate diminished global structural changes involving the calcium activation of CaM associated with aging, suggesting that there are age-related alterations in the structure of CaM. A similar reduction in the mobility of CaM isolated from senescent (26 month) brains is observed using native gels (Figure 2C).

Posttranslational Oxidative Modifications to CaM. Alterations in the primary structures of proteins isolated from aged animals have the potential to explain aspects of the loss of function characteristic of aging, and significant increases in the carbonyl content of proteins isolated from aged animals have been reported (*3*, *40*). We have, therefore, measured the average carbonyl content for CaM isolated from young (6 month) or senescent (26 month) brains, which were respectively 0.06 ± 0.02 and 0.06 ± 0.01 carbonyls/CaM. Thus, the carbonyl content in CaM does not change appreciably during aging. The small carbonyl content present in CaM suggests that there is little or no oxidative modification to a range of different amino acids, including proline, arginine, and lysine, whose oxidative modification typically can lead to the generation of carbonyl derivatives. However, since the oxidative modification of many different amino acids need not result in the production of carbonyl derivatives (*41*), we have also investigated the amino acid composition and molecular mass distribution of CaM isolated from senescent rat brain.

After base hydrolysis of CaM purified from either young (6 month) or senescent (26 month) brains, the majority of the individual amino acids in CaM were separated and identified using reversed-phase HPLC. Despite very similar amino acid compositions (Figure 3), the amino acid digest associated with CaM obtained from the aged animals contains two additional peaks relative to that from young animals with retention times of 5.4 and 14.7 min. One new peak with a retention time of 5.4 min has the same retention time as methionine sulfoxide. The area of the peak corresponding to methionine sulfoxide indicates that approximately 1.8 methionines are oxidatively modified to methionine sulfoxide. There is a corresponding reduction in the area of the peak at 9.9 min, corresponding to methionine, in CaM isolated from aged (26 month) brains.

ESI-MS Determination of the Mass Distribution of CaM. From the amino acid analysis of CaM isolated from aged (26 month) brain, it is apparent that methionine is oxidatively modified to the corresponding methionine sulfoxide (see above). However, it is unclear whether the observed oxidative modifications are randomly distributed among all CaM species or are localized within a small subpopulation of CaM species that contain multiple oxidative modifications. In addition, some posttranslational modifications (e.g., glycation) would not necessarily have been detected after the base hydrolysis used for the amino acid analysis. Therefore, to investigate other possible types of oxidative modifications and to identify the distribution of oxiforms that result from methionine oxidation, we have used ESI mass spectrometry

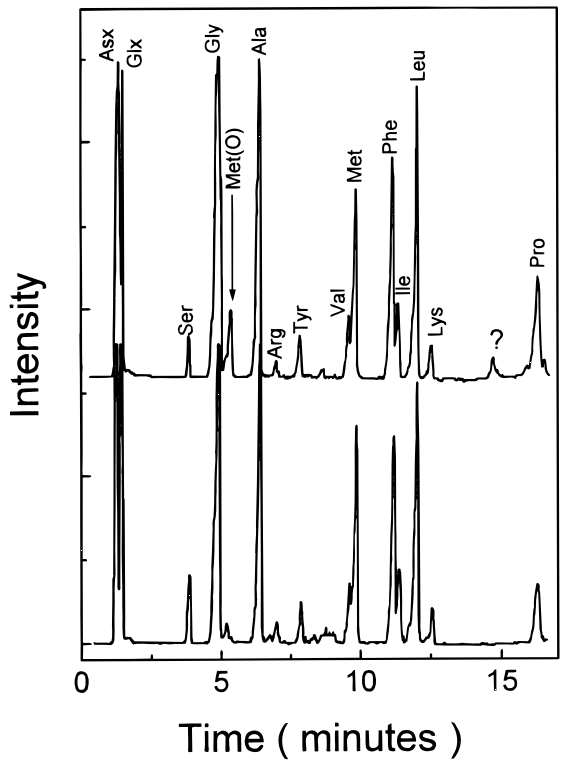

FIGURE 3: Detection of methionine sulfoxide in CaM isolated from aged brain. After hydrolysis of 6 nmol of CaM in 1 N NaOH for 16 h at 110 °C, the neutralized samples isolated from the brains of 6 (bottom) or 26 month (top) rats were derivatized with dansyl chloride, and individual amino acids were separated by reversed-phase HPLC. Excitation and emission wavelengths were 340 and 450 nm, respectively.

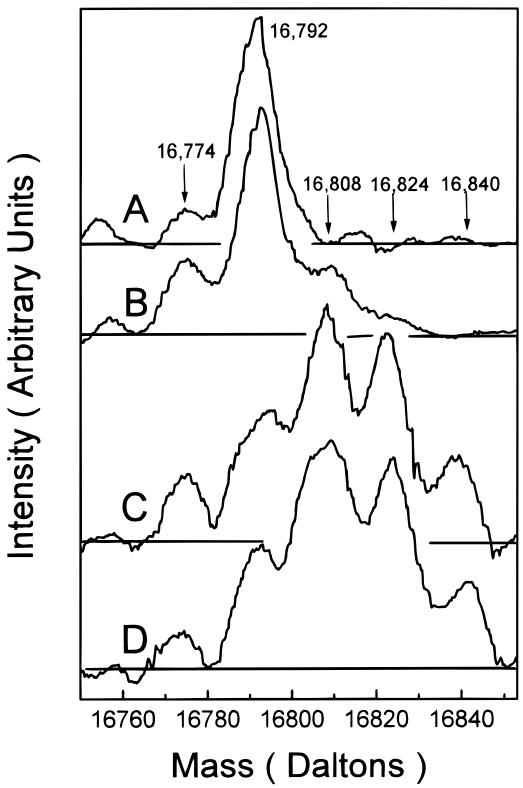

FIGURE 4: ESI-MS resolution of distribution of oxiforms in CaM after deconvolution of multiply charged ions. Spectra corresponding to CaM were isolated from the brains of 6 (A), 10 (B), 16 (C), and 26 month (D) Fischer 344 rats using experimental conditions as described in the Experimental Procedures. The associated fraction of each of these species is summarized in Figure 5. Experimentally, 1 nmol of CaM in 0.1 mM EGTA and 10 mM $(NH_4)_2CO_3$ (pH 8.6) was trapped, desalted, and then directly infused (on-line) into an Autospec EQ mass spectrometer, as described in the Experimental Procedures. Spectra were normalized to the same peak height. Relative to the integrated spectral intensity for CaM isolated from young (6 mo) brains (A), the corresponding areas are 1.5 (B), 2.8 (C), and 2.9 (D).

(ESI-MS) to resolve the molecular mass distribution of CaM species.

Using ESI-MS, we resolve two peaks for CaM isolated from young (6 month) brain, with molecular masses of 16 774 ± 3 and 16 792 ± 3 Da (Figure 4A). The latter mass corresponds to that of vertebrate CaM, whose theoretical average mass is 16 791.4 Da (*42*). The former mass represents an artifact of the conditions used to ionize CaM in the mass spectrometer, corresponding to a collision-induced dissociation (CID) product of neutral H_2O or NH_3 from CaM (*28*). Therefore, CaM purified from young (6 month) brains contains a single native isoform with no significant amount of oxidized species. In contrast, the ESI-MS spectrum for CaM isolated from any of the older animals contains additional high mass peaks at 16 808 ± 3, 16 824 ± 3, and 16 840 ± 3 Da, which correspond to additional species of CaM that differ by masses of 16, 32, and 48 Da. These higher mass CaM species are consistent with the oxidative modification of one, two, and three methionines to their corresponding methionine sulfoxides. No CaM species are apparent in any samples with a mass greater than 16 840 Da, indicating that no appreciable population of CaM species contains more than three oxidative modifications or additional posttranslational products that were not apparent from the amino acid analysis. The area of each peak in the ESI-MS spectra provides an estimate of the relative abundance of each CaM species after correction for ESI-induced fragmentation of CaM (*28*). In this manner, the distribution of oxidatively modified CaM species and the average number of oxygens incorporated in each CaM sample isolated from rats of varying ages was calculated (Figure 5). The ESI-MS spectra of CaM isolated from two different preparations of senescent (26 month) brains ($n = 6$) were virtually identical and indicate that there is an average of 1.7 ± 0.1 oxidatively modified amino acids in CaM isolated from the senescent (26 month) brain.

Distribution of Oxidatively Modified Methionines within the Primary Sequence of CaM. To identify the distribution of oxidatively modified amino acids within the primary sequence of CaM, we have used reversed-phase HPLC to separate tryptic fragments of CaM and FAB-MS to identify the associated chemical modifications (Table 1). Representative chromatograms are shown in Figure 6. We resolve eight major tryptic fragments in CaM isolated from young (6 month) brain, which contain all nine methionines (Figure 6). The relationships between the tryptic fragments and the corresponding amino acids within the primary sequence of CaM are summarized in Figure 7.

There are substantial alterations in the chromatogram of the tryptic fragments obtained from CaM isolated from the brains of senescent (26 month) animals relative to that observed in young (6 month) animals, and additional peaks are apparent at 9 and 54 min that correspond to oxidatively modified peptides of T3 and T4 (i.e., $T3_{ox}$ and $T4_{ox}$) and

Table 1: FAB-Mass Spectrometric Identification of Tryptic Fragments from Calmodulin Isolated from Young and Aged Rat Brain[a]

peak[b]	t_R (min)[c]	sequence[d]	$[M + H]^+_{theoretical}$[e]	$[M + H]^+_{experimental}$[f]
$T3_{ox}$	9.2	$Glu_{31}-(MO)-Arg_{37}$	821	821
T3	16.6	$Glu_{31}-Arg_{37}$	805	805
T5−T7	24.3	$Lys_{75}-(MO)-Arg_{86}$	1497	1498
T5−T8	27.8	$Lys_{75}-(MO)-Arg_{90}$	2000	2001
T6−T8	29.0	$Met_{76}-Arg_{90}$	1856	1855
T9	30.9	$Val_{91}-Arg_{106}$	1755	1756
T2	35.6	$Glu_{14}-Lys_{30}$	1844	1845
T1 +	37	Ala_1-Lys_{13}	1564	1564
$T10_{ox}$ +		$His_{107}-(MO)-Arg_{126}$	2418	2418
$T11_{ox}$[g]		$Glu_{127}-(MO)_2-Lys_{148}$	2522	2523
T10	42.8	$H_{107}-Arg_{126}$	2402	2401
T11	46.6	$Glu_{127}-Lys_{148}$	2490[f]	2490
$T4_{ox}$	54	$Ser_{38}-(MO)-Arg_{74}$	4087[f]	4087
T4	63	$Ser_{38}-Arg_{74}$	4072[f]	4071

[a] There were no ambiguities relating to the mass assignments of the peptide ions, and all peptides were detected with an accuracy of 0.1% of the theoretical mass of the peptide of interest. [b] Nomenclature regarding the relationship between peptides resulting from tryptic cleavage and the primary sequence of CaM is shown in Figure 7. [c] Retention times of tryptic fragments resolved by reversed-phase HPLC (see Figure 6). [d] Primary sequence corresponding to identified tryptic fragment, where MO corresponds to methionine sulfoxide. [e] Calculated masses based on monoisotopic mass distribution, except for T4 where isotopic masses are not resolved. [f] Average mass of MH^+ isotopic envelope. [g] Peptide present in small abundance.

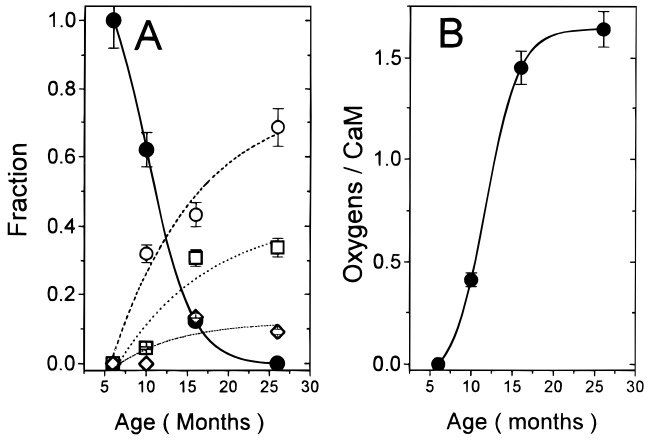

FIGURE 5: Distribution of oxidatively modified oxiforms of CaM. Fractional contribution of each species of CaM associated with native CaM (●; solid line) and oxidatively modified species containing one additional oxygen (○; dashed line), two additional oxygens (□; dotted line), and three additional oxygens (◇; short dashed line) obtained from electrospray mass spectroscopic data in Figure 4 are shown in panel A following correction for charge-induced dissociation (*28*). The average number of oxygens incorporated into each CaM species is shown in panel B, which was calculated as the sum of all CaM oxiforms multipled by the number of oxygens present. Lines are drawn for visual clarity and do not represent a physical model to describe the data.

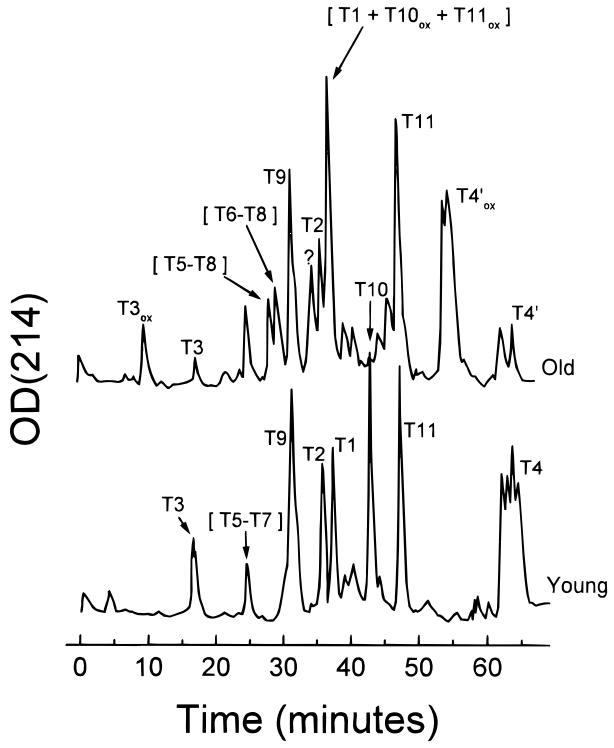

FIGURE 6: Reversed-phase HPLC resolution of tryptic peptides derived from CaM. Representative chromatograms are shown corresponding to the resolved peptides after exhaustive tryptic digestion (9 h, 37 °C) of 60 nmol of CaM isolated from the brains of 6 (bottom) or 26 month (top) Fischer 344 rats. The assignments of the parent fragments and the corresponding sulfoxides are shown with respect to the 11 expected tryptic peptides, as described in Table 1. T5−T7, T5−T8, and T6−T8 represent single peptides that were not cleaved at Lys_{76}, Lys_{78}, or Lys_{87}.

contain methionine sulfoxide (Figure 6; Table 1). In addition, there are large decreases in the intensity of the parent peaks associated with T3 (t_R = 17 min), T10 (t_R = 43 min), and T4 (t_R = 63 min). The oxidation product of T10 (i.e., $T10_{ox}$) has a retention time of 37 min and overlaps with T1. Upon separation of these parent peptides (T3, T4, and T10) and selective in vitro oxidation of the corresponding methionine residues, identical retention times are observed that correspond to the oxidation products observed in CaM isolated from senescent brain (i.e., $T3_{ox}$, $T4_{ox}$, and $T10_{ox}$), indicating that methionines at positions throughout the primary sequence of CaM are selectively oxidized during aging. There is a small amount of a peptide whose mass corresponds to that of an oxidation product of T11 with a retention time of 37 min that overlaps with that of T1 and $T10_{ox}$; however, there is little or no reduction in the area associated with the parent peak associated with T11 (t_R = 47 min). This latter result is in sharp contrast to previous in vitro results where methionines located at the carboxyl-terminus (i.e., T11) were highly sensitive to oxidative modification using either H_2O_2 or $ONOO^-$ (*9*, *10*). Thus, while multiple methionines are selectively oxidized to the corresponding methionine sulfoxide in CaM isolated from aged brain or using in vitro oxidants (i.e., H_2O_2 or $ONOO^-$), the pattern of methionine oxidation is markedly different in

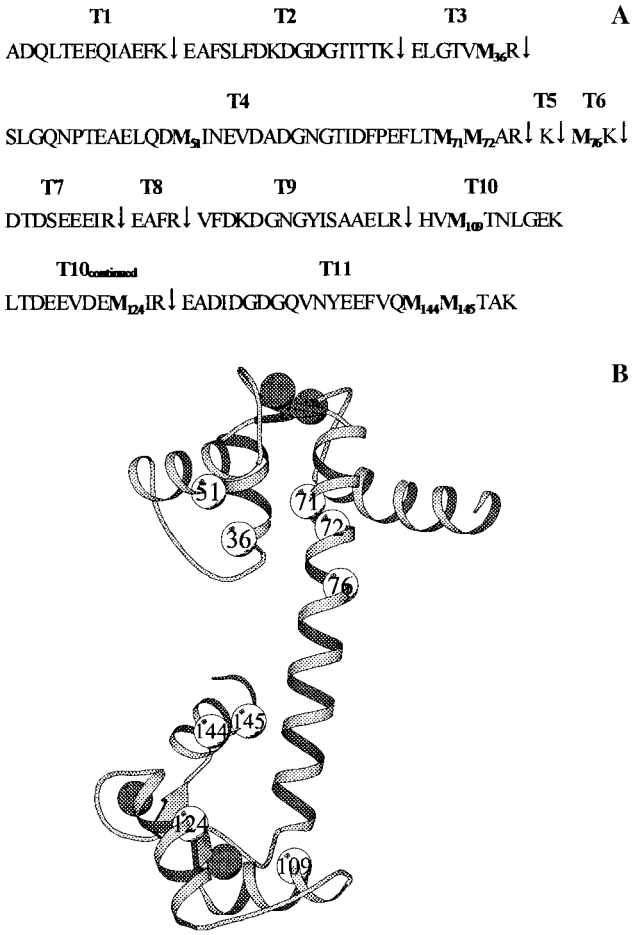

FIGURE 7: Positions of methionines within calmodulin. (A) Locations of the nine methionines within the primary sequence of vertebrate CaM relative to observed tryptic cleavage sites (↓) are indicated, where the 11 expected tryptic fragments are indicated by the letter T followed by a number. (B) The relative positions of the nine methionines within the tertiary structure of CaM are highlighted in the ribbon drawing of the backbone fold of the calcium saturated form of CaM. The coordinates are taken from Brookhaven Protein Data Bank file 1cll.pdb (*68*), and the drawing was constructed using the program MolScript (*69*). Shaded circles represent calcium ligands.

vivo relative to that observed in vitro. These latter results suggest that the ROS involved in the oxidative modification of CaM under physiological conditions have a different selectivity relative to that observed in vitro using H_2O_2 or $ONOO^-$. Alternatively, CaM isolated from senescent brain could represent a fraction of the oxidatively modified CaM species that were initially modified, which may not have been subjected to intracellular repair or degradation.

The presence of multiple methionines in tryptic peptides T4 and T10 precludes a quantitative determination of the exact positions of the oxidatively modified methionines located in these proteolytic fragments. However, in no instance are there substantial amounts of any peptide containing multiple methionine sulfoxides apparent in the FAB-MS spectra, suggesting that in the majority of instances that there is a single methionine sulfoxide present in the oxidatively modified peptides. Thus, the observed decreases in the apparent areas of the parent peptides T3, T4, and T10 permit an estimation of the average extent of oxidative modification, which corresponds to approximately 2.2 ± 0.3 methionine sulfoxides/CaM.

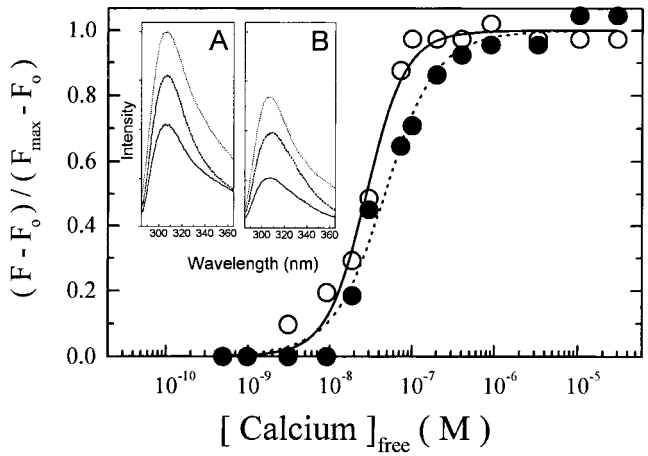

FIGURE 8: Calcium-dependent structural changes associated with activation of CaM. Calcium-dependent fluorescence intensity changes, $[|(F - F_o)/(F_{max} - F_o)|]$, for CaM isolated from 6 (○) and 26 month (●) brains, where F is the observed fluorescence intensity (λ_{em} = 306 nm) associated with Tyr_{99} and Tyr_{138} (see inset). F_o and F_{max} are the fluorescence intensities of apo- and calcium-saturated CaM. Solid (6 month) and dotted (26 month) lines represent the best fits to eq 1 (see Experimental Procedures). ΔG_1 (6 month) = −9.3 ± 0.5 kcal mol^{-1}, ΔG_2 (6 month) = −20.6 ± 0.1 kcal mol^{-1}, and ΔG_c (6 month) = −2.8 ± 0.5 kcal mol^{-1}. ΔG_1 (26 month) = −9.9 ± 0.5 kcal mol^{-1}, ΔG_2 (26 month) = −20.0 ± 0.1 kcal mol^{-1}, and ΔG_c (26 month) = −1.0 ± 0.2 kcal mol^{-1}. Inset corresponds to fluorescence emission spectra for CaM isolated from 6 (A) or 26 month (B) brain in the presence of 0.1 mM EGTA (solid line), 0.1 mM free calcium (dashed line), or the addition of 27 μM CaMKII20 target peptide (dotted line). Sample conditions include 18 μM CaM in 0.1 M KCl, 1 mM $MgCl_2$, 0.1 mM EGTA, and 0.1 M HEPES (pH 7.5). Calcium was added to yield the desired free concentration and was directly measured using FURA-2, as previously described (*20*). Excitation was at 275 nm, using a Coherent Innova 400 laser. Fluorescence emission spectra were detected using a single grating Jovin Yvon monochromoter with a 4-nm slit width. Errors in the fluorescence measurements were less than 1% of the indicated values.

Changes in Intrinsic Tyrosine Fluorescence upon Calcium Activation and Peptide Binding. The intrinsic fluorescence associated with Tyr_{99} and Tyr_{138} provides a convenient measurement of the structure of CaM in the vicinity of calcium binding sites 3 and 4 (*43*, *44*). We have therefore compared the fluorescence intensity characteristic of apo-CaM with that of calcium-activated CaM free in solution or bound to a peptide corresponding to the CaM binding site of CaM-dependent protein kinase (CaMKII20) for CaM isolated from either young (6 month) or senescent (26 month) brains (Figure 8, inset). Irrespective of the CaM source, there is a substantial increase in the fluorescence intensity of CaM upon calcium activation, which further increases upon peptide binding. The fluorescence intensity under all conditions is lower for CaM isolated from senescent brains relative to the young brains under the same experimental conditions. One observes a similar decrease in the average lifetime of the tyrosines in CaM isolated from senescent brain relative to young controls (data not shown), indicating that there are appreciable structural changes in CaM isolated from senescent brain that may result from either differences in the tertiary structures of CaM or from alterations in specific quenching interactions in the vicinity of these tyrosines in calcium binding sites III and IV. Regardless of the physical reason for the calcium-dependent change in intrinsic fluorescence, the ability to detect calcium-dependent structural

changes using these fluorescence intensity changes permits an assessment of possible differences in either the calcium affinity or cooperativity for CaM isolated from young and senescent brains.

Loss of Cooperative Structural Changes Associated with Calcium Activation. CaM isolated from either young or senescent brains exhibits an increase in the intrinsic fluorescence intensity associated with calcium binding, where the respective calcium concentrations necessary for the half-maximal fluorescence enhancement are 29 and 47 nM (Figure 8). Similar structural changes in the vicinity of calcium binding loop 4 are observed in wheat CaM (*20*), suggesting that the calcium-binding sites in the carboxyl-terminal domain of CaM have a high calcium affinity. The larger amount of calcium necessary to observe the fluorescence enhancement in CaM isolated from senescent brains could be related to either a lower calcium binding affinity or a reduced cooperativity between the high affinity calcium binding sites. Fitting the data to eq 1 in the Experimental Procedures indicates that there is no difference in the apparent calcium binding affinities for CaM isolated from young or senescent brain. However, the highly cooperative interaction between the high-affinity calcium binding sites in CaM isolated from young brains ($\Delta G_c = -2.8 \pm 0.5$ kcal mol^{-1}) is markedly reduced in CaM isolated from senescent brains ($\Delta G_c = -1.0 \pm 0.2$ kcal mol^{-1}). The decreased cooperativity suggests that oxidative modifications within the primary sequence of CaM disrupt the structural coupling between high affinity calcium binding sites that are normally associated with calcium activation.

Measurement of Calcium-Binding Stoichiometries. We have directly measured the stoichiometry of calcium binding for CaM isolated from young and senescent brains to address the possibility that alterations in the cooperative interactions between the high affinity binding sites could result from the disruption of a single high affinity calcium binding site. CaM isolated from young (6 month) and senescent (26 month) brain respectively bind 3.74 ± 0.10 and 3.33 ± 0.11 calcium ions/mol of CaM. The observed binding stoichiometries are consistent with the presence of the four high affinity calcium-binding sites in CaM (*44*). The small apparent decrease in the amount of bound calcium in CaM isolated from aged brains is not statistically significant ($p > 0.05$) and indicates that the majority of CaM species present in both young and senescent brain contain four high affinity calcium-binding sites.

Global Structural Changes within CaM Associated with Calcium Binding. Due to the sensitivity of the quantum yield of tyrosine to local environmental changes, the age-dependent decrease in the fluorescence intensity associated with Tyr_{99} and Tyr_{138} in CaM may result from either small structural alterations that modulate specific quenching interactions or could result from global alterations in the structure of CaM that modulate the accessibility to aqueous solvent (*45*). Therefore, to determine whether there are substantial age-related structural differences around Tyr_{99} and Tyr_{138}, we have measured the average solvent accessibility of these tyrosines to the water-soluble quencher TEMPAMINE (Figure 9). The solvent accessibility increases upon calcium activation for CaM isolated from young (6 month) brain, where the Stern−Volmer quenching constant (K_{sv}) increases from 0.51 ± 0.02 for apo-CaM to 0.62 ± 0.04 for calcium-activated CaM and is consistent with other results indicating a more open tertiary structure within each of the opposing globular domains in CaM upon calcium activation (*20*, *46*, *47*). For CaM isolated from senescent brain, the tyrosines are more exposed and do not exhibit calcium-induced changes in their solvent accessibility; the Stern−Volmer quenching constant (K_{sv}) is 0.70 ± 0.03 for apo-CaM and 0.68 ± 0.04 for calcium-activated CaM. Thus, age-related structural changes result in more solvent exposure of Tyr_{99} and Tyr_{138}, consistent with the reduced mobility observed by SDS−PAGE, and diminished sensitivity to calcium binding of CaM isolated from aged brain relative to young controls (Figure 2). The lack of any change in the solvent accessibility of Tyr_{99} and Tyr_{138} in CaM isolated from senescent brains upon calcium activation is further evidence indicating that the long-range structural coupling normally apparent between the high affinity calcium binding sites in the carboxyl-terminus of CaM isolated from the brains of young animals is diminished.

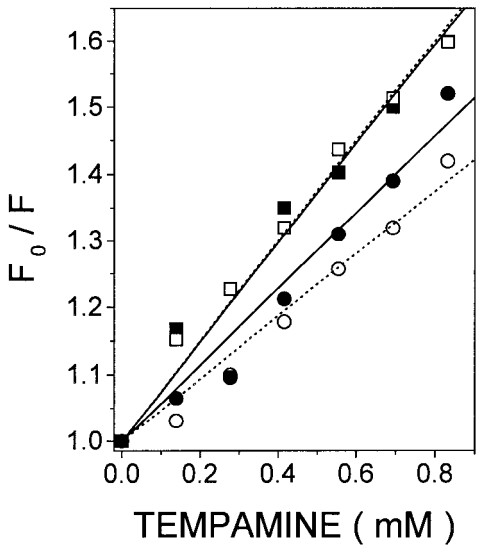

FIGURE 9: Enhanced solvent accessibility in CaM isolated from aged brain. The apparent Stern-Volmer (K_{sv}) quenching constants for Tyr_{99} and Tyr_{138} to the water soluble-quencher TEMPAMINE were determined in the presence of either 0.1 mM $CaCl_2$ (●, ■) or 0.1 mM EGTA (○, □) for 6 μM CaM in 0.1 M KCl, 1 mM $MgCl_2$, and 0.1 M HEPES (pH 7.5) at 25 °C. CaM samples were isolated from the brains of 6 (○, ●) or 26 month (□, ■) rats. Lines represent the best fit to the Stern−Volmer equation (*27*). For CaM isolated from 6 month old rat brain, $K_{sv}(EGTA) = 0.51 \pm 0.02$ M^{-1} s^{-1}, and $K_{sv}(Ca^{2+}) = 0.62 \pm 0.04$ M^{-1} s^{-1}. For CaM isolated from 26 month old rat brain, $K_{sv}(EGTA) = 0.70 \pm 0.03$ M^{-1} s^{-1} and $K_{sv}(Ca^{2+}) = 0.68 \pm 0.04$ M^{-1} s^{-1}. Errors in the fluorescence measurements were less than 1% of the indicated values.

Fluorescence Intensity Changes of Trp_4 in the CaM-Binding Sequence of the PM-Ca-ATPase upon CaM Binding. Trp_4 in the peptide corresponding to the CaM-binding sequence of the PM-Ca-ATPase (i.e., C28W) is generally thought to be a critical recognition site that facilitates the productive interaction between CaM and the PM-Ca-ATPase that results in enzyme activation (*33*). Upon binding to CaM isolated from young (6 month) brains, a 5 nm blue-shift in the emission spectrum accompanied by a 54% reduction in the fluorescence intensity of Trp_4 is observed (Figure 10, inset). These spectral changes suggest a more hydrophobic environment around Trp_4 as a result of peptide binding, consistent with the earlier suggestion that Trp_4 is an important

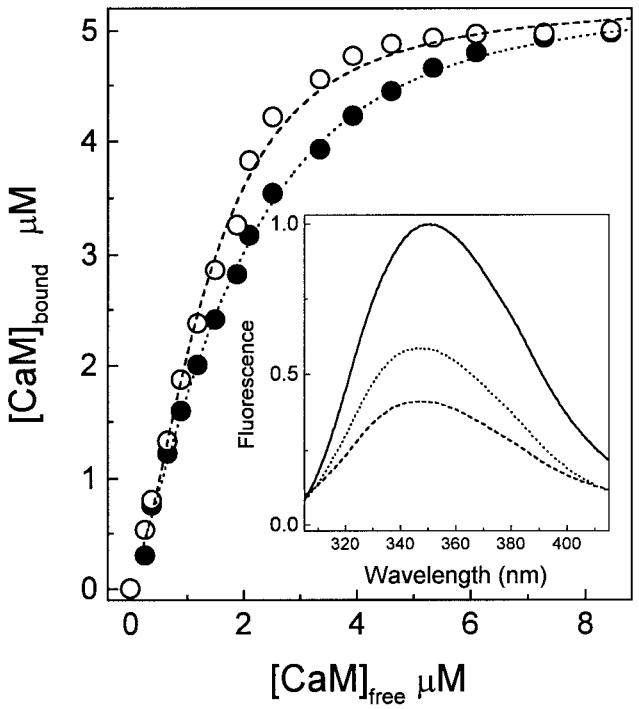

FIGURE 10: Titration of CaM with target peptide C28W derived from the PM-Ca-ATPase. CaM binding was measured using the decrease in the fluorescence intensity of Trp_4 in 5 μM C28W upon binding CaM isolated from 6 (○) or 26 month (●) rat brains (λ_{ex} = 295 nm; λ_{em} = 350 nm), as previously described (*9*). Data were analyzed using eq 2, as described in Experimental Procedures, to calculate binding energies for CaM isolated from 6 and 26 month brains, which were as follows: ΔG_1 (6 month) = -8.5 ± 0.2 kcal mol^{-1} and ΔG_2 (6 month) = -7.4 ± 0.2 kcal mol^{-1}; ΔG_1 (26 month) = -8.7 ± 0.2 kcal mol^{-1} and ΔG_2 (26 month) = -6.5 ± 0.2 kcal mol^{-1}. Age-related changes in binding energies are $\Delta\Delta G_1 = -0.2 \pm 0.3$ kcal mol^{-1} and $\Delta\Delta G_2 = -0.9 \pm 0.3$ kcal mol^{-1}. Inset: Fluorescence emission spectra of C28W alone (solid line) or for C28W in the presence of 15 μM CaM isolated from either 6 (dashed line) or 26 month (dotted) brains. Experimental buffer contained 0.1 M KCl, 1 mM $MgCl_2$, 0.1 mM $CaCl_2$, and 0.1 M HEPES (pH 7.5) in the presence of 5 μM C28W at 25 °C. Errors in the fluorescence measurements were less than 1% of the indicated values. Errors in the determination of the concentrations of free and bound CaM were propagated and are approximately 0.3 μM.

recognition site between multiple methionines located in the carboxyl-terminal domain of CaM (i.e., Met_{109}, Met_{124}, Met_{144}, and Met_{145}) that participate in facilitating the productive binding of the carboxyl-terminus of CaM to the PM-Ca-ATPase (*32*, *33*, *48*).

There is a 42% reduction in the fluorescence intensity of Trp_4 in C28W upon binding CaM isolated from senescent brain, corresponding to a 22% decrease in the maximal fluorescence intensity change of Trp_4 observed when CaM isolated from young (6 month) brains binds to C28W (see above). The smaller change in fluorescence intensity of Trp_4 suggests that there are conformational differences in CaM that alter its interaction with C28W in the vicinity of Trp_4. This reduction corresponds to a similar reduction in the maximal velocity associated with the CaM-dependent activation of the PM-Ca-ATPase, suggesting that a subpopulation of CaM species is unable to activate the PM-Ca-ATPase as a result of incorrect binding to C28W. Alternatively, the smaller spectral change may be the average of a range of altered binding interactions between the oxidatively modified CaM species and C28W, which result in alterations in either specific binding interactions between different CaM species around Trp_4 or the conformation of the bound peptide.

Binding Affinity of CaM to the PM-Ca-ATPase. To investigate possible differences in the binding interaction between CaM and the PM-Ca-ATPase, we have used the fluorescence intensity changes associated with Trp_4 in C28W that result from CaM binding to measure alterations in the affinities between the carboxyl- and amino-terminal domains of CaM and C28W (see above). In comparison to CaM isolated from young (6 month) brains, more CaM is necessary to observe the maximal fluorescence intensity change associated with binding to C28W when CaM is isolated from senescent brains (Figure 10). These results indicate that CaM isolated from senescent brains has a reduced binding affinity to the PM-Ca-ATPase. One observes a similar reduction in the binding affinity between CaM isolated from senescent brains and a peptide corresponding to the CaM-binding sequence of CaM-dependent protein kinase II (data not shown), suggesting that age-dependent alterations in the binding affinity of CaM to target proteins may result in the modulation of a broad range of enzyme activities.

A quantitative description of the binding affinities between CaM isolated from young (6 month) and senescent (26 month) brains and C28W requires that both of the binding sites within CaM be considered (see eq 2 in Experimental Procedures). For CaM isolated from young brain, the dissociation constants associated with the two CaM binding domains differ by an order of magnitude [K_{d1} (young) = $0.6 \pm 0.2 \times 10^{-6}$ M; K_{d2} (young) = $4 \pm 1 \times 10^{-6}$ M] and respectively correspond to the binding affinity of the carboxyl- and amino-terminal domains of CaM for C28W (*9*). The apparent affinity of the carboxyl-terminal domain in CaM isolated from senescent brain is very similar to that of native CaM [i.e., K_{d1} (old) = $0.4 \pm 0.2 \times 10^{-6}$ M], while that associated with the amino-terminal domain is reduced by approximately 40-fold [K_{d2} (old) = $16 \pm 8 \times 10^{-6}$ M]. Since these values represent average values that assume CaM isolated from senescent brains can be treated as a homogeneous population, the actual binding affinities associated with the subpopulation of CaM species that do not fully activate the PM-Ca-ATPase may be smaller.

Secondary Structure of CaM. Possible age-related differences in the secondary structure of CaM were assessed using CD spectroscopy to estimate the apparent α-helical content of CaM isolated from young (6 month) and senescent (26 month) brains. CD spectra were measured between 200 and 240 nm at 1 nm intervals. The CD spectrum obtained from CaM isolated from senescent brains at 20 °C is substantially different from that of native CaM isolated from young brains (Figure 11), suggesting that these samples have different average secondary structures. There is a small but reproducible age-dependent decrease in apparent α-helical content, which decreases from 63 ± 1% for native CaM to 59 ± 1% for CaM isolated from senescent brains. The decreased α-helical content in CaM isolated from senescent brain relative to that isolated from young brains indicates that the oxidative modification of methionine to its methionine sulfoxide disrupts protein secondary structural elements and may explain the diminished structural coupling apparent in CaM isolated from aged tissue (see above).

Thermal Stability of CaM. CD spectra associated with CaM isolated from young and senescent brains were

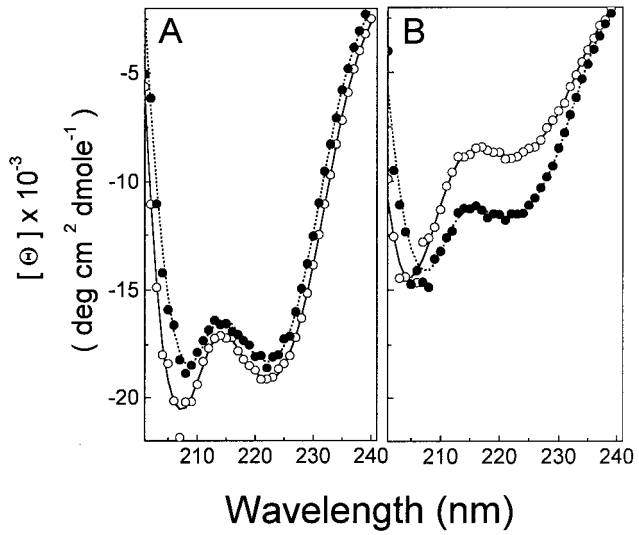

FIGURE 11: Secondary structure of calcium-saturated CaM. CD spectra obtained using CaM isolated from brains of 6 (○; solid line) and 26 month (●; dotted line) brains at 20 (A) and 70 °C (B). Lines represent the least-squares fit to the CD spectra obtained using the program Contin (*29*). For CaM at 20 °C, the calculated α-helical content was 63% (○) and 59% (●). At 70 °C, the calculated α-helical content was 33% (○) and 41% (●). Experimental errors associated with the experimental determination of the α-helical content of CaM were approximately 1%. Desalted CaM (6 μM) was dissolved in 10 mM Tris-HCl (pH 7.5), 0.1 M $KClO_4$, 1 mM $Mg(ClO_4)_2$, and 0.1 mM $Ca(ClO_4)_2$.

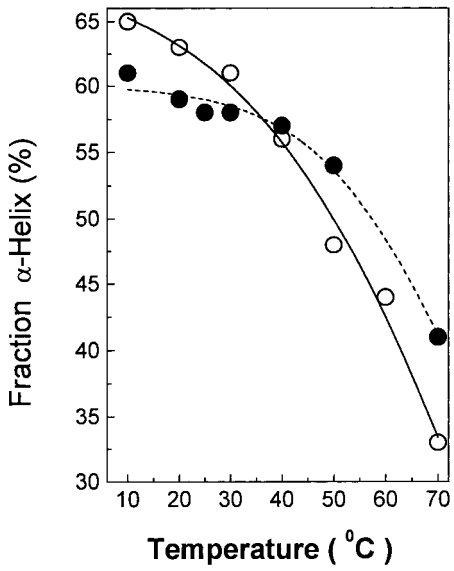

FIGURE 12: Thermal stability of CaM isolated from young and aged brains. Temperature dependence of the apparent α-helical content associated with CaM isolated from the brains of 6 (○; solid line) and 26 month (●; dashed line) old rats. Sample conditions are as described in legend to Figure 11. Errors in the determination of the α-helical content were approximately 1% of the indicated values.

measured at 10 °C intervals between 10° and 70 °C (Figure 12), and the α-helical content was calculated (see above). At 70 °C, larger spectral differences are observed in the CD spectra (Figure 11B); CaM isolated from senescent brain has a higher α-helical content (i.e., 41% α-helix) in comparison to that associated with CaM isolated from young brain (i.e., 33% α-helix). The estimated half-point of thermal denaturation associated with the secondary structure for CaM isolated from young brains occurs at 71 ± 3 °C, whereas that for CaM isolated from senescent brains occurs at 84 ± 3 °C (Figure 12). The 13 ± 4 °C increase in the thermal stability of CaM isolated from senescent relative to young brains suggests that methionine sulfoxides present in CaM isolated from aged brain disrupts long-range structural interactions that normally facilitate the cooperative unfolding of CaM. The greater thermal stability associated with CaM isolated from senescent brains is consistent with the reduced mobility of CaM on SDS−PAGE, since CaM isolated from senescent brains would be expected to have more residual structure. A simple two-state model that assumes a highly cooperative temperature-dependent denaturation of the α-helices in CaM permits the calculation of the stabilization of the native structure associated with CaM isolated from senescent brains (see eq 3 in Experimental Procedures) and suggests that the oxidative modification of selected methionines during aging results in a 0.5 ± 0.1 kcal mol^{-1} *increase* in thermal stability.

DISCUSSION

There are secondary and tertiary structural changes in aged CaM that disrupt global structural transitions associated with calcium activation (Figures 2, 8, and 9). These latter structural alterations correlate with the oxidative modification of multiple methionines in CaM isolated from aged brains (Figure 3) and result in an impaired ability to activate the PM-Ca-ATPase (Figure 1). Methionine oxidation is progressive with age (Figure 4), resulting in a decreased affinity of one binding domain of CaM_{ox} toward the PM-Ca-ATPase (see legend in Figure 10). Age-related structural and functional alterations involving oxidatively modified CaM (CaM_{ox}) are consistent with the higher basal levels of calcium and longer calcium transients observed in cells isolated from aged tissue (*14*, *49*, *50*) and suggest that the oxidative modification of selected methionines in CaM_{ox} may explain the mechanism of inhibition involving some calcium regulatory proteins associated with aging (see below).

Differential Kinetic Effects Associated with Methionine Oxidation. Consistent with the important role of the majority of methionines in CaM in providing a high affinity binding surface in the activation of target proteins (*51*−*54*), it has previously been observed that the in vitro oxidative modification of methionines in CaM results in a decreased ability of CaM_{ox} to activate cyclic nucleotide phosphodiesterase, adenylate cyclase, nitric oxide synthase, and the PM-Ca-ATPase (*6*−*10*). In the case of the PM-Ca-ATPase, substantial differences in the extent of inhibition have been observed depending on the distribution of oxidatively modified methionines (*55*). The oxidation of the majority of the methionine residues in CaM alter only the binding affinity between CaM_{ox} and the PM-Ca-ATPase (*9*, *28*). In contrast, the oxidation of methionines located in the carboxyl-terminal domain of CaM has been shown to disrupt the long-range structural coupling between the opposing globular domains that normally accompany calcium activation and permit the productive association between CaM and target proteins (*9*, *28*). These results suggest that the shift in the CaM-dependent activation of the PM-Ca-ATPase [i.e., $(CaM)_{1/2}$] toward higher concentrations of CaM results from the reduced affinity between CaM_{ox} and the PM-Ca-ATPase, while the decrease in the maximal CaM-dependent activation of the PM-Ca-ATPase (i.e., V_{max}) by CaM_{ox} is the result of global structural changes that result in an altered and

nonproductive interaction with the CaM-binding sequence of the PM-Ca-ATPase that results in a reduction in the CaM-dependent activation of the PM-Ca-ATPase (Figure 1). These results are consistent with earlier measurements where the in vitro oxidative modification of methionines located at the carboxyl-terminus of CaM were shown to result in a substantial reduction in V_{max} as a result of global structural alterations involving the disruption of the structural coupling between the opposing globular domains of CaM (*28*).

Functional Alterations in CaM-Dependent Enzymes During Aging. While previous measurements have not identified age-related alterations in the function of CaM, reported reductions in the activity of the PM-Ca-ATPase and CaM-dependent protein kinase II isolated from the brains of older animals could be the result of decreased expression levels or oxidative modifications involving CaM (*56*−*60*). Similar reductions in the transport activity of the PM-Ca-ATPase in aged erythrocytes are reversed upon purification of the erythrocyte ghosts and addition of exogenous CaM (*61*, *62*), suggesting that CaM itself may be a principal target of ROS under conditions involving oxidative stress.

Physiological Relevance of Methionine Oxidation. Methionine and cysteine are the only amino acids that can be repaired following their oxidative modification by intracellular reductases found in all organisms (*3*). Therefore, the reversible oxidative modification of these residues provides a possible regulatory mechanism that may modulate intracellular metabolism and has the potential to enhance the ability of cells to survive oxidative insults (*4*, *5*). While it currently remains unclear if the primary role of methionine sulfoxide reductase (MsrA) involves (i) the maintenance of the necessary amount of methionine to allow protein synthesis or (ii) the repair of oxidatively modified proteins, strains of yeast that lack MsrA have an increased sensitivity to oxidative stress (*63*). Thus, the ability to repair oxidatively modified methionine residues is critical to the cellular ability to survive oxidative insults.

Methionines are themselves rarely involved in catalysis, and their oxidative modification frequently results in little or no alteration in enzymatic function. Thus, eight nonessential and readily oxidizable methionines are found near the active site of glutamine synthetase that when oxidized do not perturb function (*5*). Therefore, methionine has been suggested to function as an endogeneous antioxidant that protects essential and nonrepairable amino acids from oxidative modification (*3*, *5*). However, the flexible, nonpolar side chain of methionine has also been suggested to provide the necessary conformational flexibility for the rapid binding interactions necessary between proteins involved in signal transduction (*64*, *65*). Thus, essentially all nine methionines in CaM are involved in binding to target proteins, and methionine side chains represent nearly half the total binding surface (*51*−*54*). Therefore, the oxidative modification of the nonpolar thioether in methionine to the corresponding sulfoxide will dramatically increase the polarity of the binding sites and is expected to modulate the interactions between CaM and a broad range of target proteins, including the PM-Ca-ATPase (see above). Furthermore, since the productive interaction between CaM and target proteins is thought to involve an ordered binding mechanism in which association of the carboxyl-terminal domain establishes the correct geometry for association with the amino-terminal domain (*66*, *67*), alterations in the relative affinity or specificity of the carboxyl-terminal domain for its binding site has the potential to interfere with the normal binding mechanism necessary for enzyme activation.

Conclusions. Multiple methionines are oxidatively modified in CaM during biological aging, resulting in global structural changes and a decreased ability to activate the PM-Ca-ATPase. These structural alterations in CaM provide a possible mechanism for the observed loss of calcium regulation during aging. The inhibition of the PM-Ca-ATPase and other target proteins by CaM_{ox} has the potential to facilitate cellular survival under conditions of oxidative stress by minimizing ATP utilization. Direct physical measurements of the nonproductive complex between oxidatively modified CaM and the CaM-binding sequence of the PM-Ca-ATPase will be necessary to further define the mechanism of inhibition of the PM-Ca-ATPase by CaM isolated from senescent brain further.

ACKNOWLEDGMENT

We thank Diana J. Bigelow and Deborah A. Ferrington for insightful discussions and Ms. Homigol Biesiada of the KU Mass Spectrometry Laboratory for her efforts in acquiring the FAB and ESI spectra. This work is dedicated to Murphy's Law.

REFERENCES

1. Stadtman, E. R., Starke-Reed, P. E., Oliver, C. N., Carney, J. M., and Floyd, R. A. (1992) *EXS 62*, 64−72.
2. Gafni, A. (1997) *J. Am. Geriatr. Soc. 45*, 871−880.
3. Berlett, B. S., and Stadtman, E. R. (1997) *J. Biol. Chem. 272*, 20313−20316.
4. Vogt, W. (1995) *Free Radical Biol. Med. 18*, 93−105.
5. Levine, R. L., Mosoni, L., Berlett, B. S., and Stadtman, E. R. (1996) *Proc. Natl. Acad. Sci. U.S.A. 93*, 15036−150540.
6. Walsh, M., and Stevens, F. C. (1977) *Biochemistry 16*, 2742−2749.
7. Wolff, J., Cook, G. H., Goldhammer, A. R., and Berkowitz, S. A. (1980) *Proc. Natl. Acad. Sci. U.S.A. 77*, 3841−3844.
8. Carafoli, E., Krebs, J., and Chiesi, M. (1988) in *Calmodulin* (Cohen, P., and Klee, C. B., Eds.) pp 297−312, Elsevier, New York.
9. Yao, Y., Yin, D., Jas, G., Kuczera, K., Williams, T. D., Schöneich, Ch., and Squier, T. C. (1996) *Biochemistry 35*, 2767−2787.
10. Hühmer, A. F. R., Gerber, N. C., Ortiz de Montellano, P. R., and Schöneich, Ch. (1996) *Chem. Res. Toxicol. 9*, 484−491.
11. Carafoli, E. (1991) *Physiol. Rev. 71*, 129−153.
12. Meissner, G. (1994) *Annu. Rev. Physiol. 56*, 485−508.
13. Kukreja, R. C., and Hess, M. L. (1992) *Cardiovasc. Res. 26*, 641−655.
14. Kirischuk, S., and Verkhratsky, A. (1996) *Life Sci. 59*, 451−459.
15. Michaelis, M. L., Bigelow, D. J., Schöneich, Ch., Williams, T. D., Ramonda, L., Yin, D., Hühmer, A. F. R., Yao, Y., Gao, J., and Squier, T. C. (1996) *Life Sci. 59*, 405−412.
16. Niggli, V., Penniston, J. T., and Carafoli, E. (1979) *J. Biol. Chem. 254*, 9955−9958.
17. Strasburg, G. M., Hogan, M., Birmachu, W., Thomas, D. D., and Louis, C. F. (1988) *J. Biol. Chem. 263*, 542−548.
18. Klee, C. B., and Vanaman, T. C. (1982) *Adv. Protein Chem. 35*, 213−321.
19. Lanzetta, P. A., Alverez, L. J., Reinsch, P. S., and Candia, O. (1979) *Anal. Biochem. 100*, 95−97.
20. Yao, Y., Schöneich, Ch., and Squier, T. C. (1994) *Biochemistry 33*, 7797−7810.
21. Gornal, A., Bardawill, C., and David, M. (1949) *J. Biol. Chem. 177*, 751−766.

22. Wang, H., Kumar, K. N., and Michaelis, E. K. (1992) *Neuroscience 46*, 793−806.
23. Levine, R. L., Garland, D., Oliver, C. N., Amici, A., Climent, I., Lenz, A., Ahn, B., Shaltied, S., and Stadtman, E. R. (1990) *Methods Enzymol. 186*, 464−478.
24. Trybus, K. M., and Lowey, S. (1985) *J. Biol. Chem. 260*, 15988−15995.
25. Laemmli, U. K. (1970) *Nature 227*, 680−685.
26. Burgess, W. H., Jemiolo, D. K., and Kretsinger, R. H. (1980) *Biochim. Biophys. Acta 623*, 257−270.
27. Lehrer, S. S., and Leavis, P. C. (1978) *Methods Enzymol. 49*, 222−236.
28. Gao, J., Yin, D. H., Yao, Y., Sun, H., Qin, Z., Schöneich, Ch., Williams, T. D., and Squier, T. C. (1998) *Biophys. J. 74*, 1115−1134.
29. Venyaminov, S. Y., and Yang, J. T. (1996) in *Circular Dichroism and the Conformational Analysis of Biomolecules* (Fasman, G. D., Ed.) pp 69−107, Plenum Press, New York.
30. Pedigo, S., and Shea, M. A. (1995) *Biochemistry 34*, 1179−1196.
31. Matthews, J. C. (1993) *Fundamentals of Receptor, Enzyme, and Transport Kinetics*, CRC Press, Boca Raton.
32. Chapman, E. R., Alexander, K., Vorherr, T., Carafoli, E., and Storm, D. R. (1992) *Biochemistry 31*, 12819−12825.
33. Crivici, A., and Ikura, M. (1995) *Annu. Rev. Biophys. Biomol. Struct. 24*, 85−116.
34. Press, W. H., Flannery, B. P., Teukolsky, S. A., and Vetterling, W. T. (1988) *Numerical Recipes in C, The Art of Scientific Computing*, Cambridge University Press, New York.
35. Becktel, W. J., and Schellman, J. A. (1987) *Biopolymers 26*, 1859−1877.
36. Coleman, P., Finch, C., and Joseph, J. (1990) *Neurobiol. Aging 11*, 1−2.
37. Strehler, E. E., and Roger, M. S. (1996) in *Guidebook to the Calcium Binding Proteins* (Celio, M. R., Pauls, T., and Schwaller, B., Eds.) pp 34−40, Oxford University Press, Oxford.
38. Klee, C. B., Crouch, T. H., and Krinks, M. H. (1979) *Proc. Natl. Acad. Sci. U.S.A. 76*, 6270−6273.
39. Zhang, M., Li, M., Wang, J. H., and Vogel, H. J. (1994) *J. Biol. Chem. 269*, 15546−15552.
40. Harman, D. (1987) in *Modern Biological Theories of Aging* (Butler, R. N., Schneider, E. L., Sprott, R. L., and Warner, H. R., Eds) pp 81−87, Raven Press, New York.
41. Stadtman, E. R. (1993) *Annu. Rev. Biochem. 62*, 797−821.
42. Simmen, R. C. M., Tanaka, T., Ts'ui, K. F., Putkey, J. A., Scott, M. J., Lai, E. C., and Means, A. R. (1985) *J. Biol. Chem. 260*, 907−912.
43. Wang, C.-L. A., Aquaron, R. R., Leavis, P. C., and Gergely, J. (1982) *Eur. J. Biochem. 124*, 7−12.
44. Babu, Y. S., Sack, J. S., Greenough, T. J., Bugg, C. E., Means, A. R., and Cook, W. J. (1985) *Nature 315*, 37−40.
45. Ross, J. B. A., Laws, W. R., Rousslang, K. W., and Wyssbrod, H. R. (1992) in *Topics in Fluorescence Spectroscopy*, Vol. 3, (Lakowicz, J. R., Ed.) pp 1−63, Plenum Press, New York.
46. Kuboniwa, H., Tjandra, N., Grzesiek, S., Ren, H., Klee, C. B., and Bax, A. (1995) *Nat. Struct. Biol. 2*, 768−776.
47. Tjandra, N., Kuboniwa, H., Ren, H., and Bax, A. (1995) *Eur. J. Biochem. 230*, 1014−1024.
48. Vorherr, T., James, P., Krebs, J., Enyedi, A., McCormick, D. J., Penniston, J. T., and Carafoli, E. (1990) *Biochemistry 29*, 355−365.
49. Peterson, C. (1992) in *Aging and Cellular Defense Mechanisms*. (Franceschi, C., Crepaldi, G., Cristofalo, V. J., and Vijg, J., Eds.) *N.Y. Acad. Sci. 663*, 279−293.
50. Chaudière, J. (1994) in *Free Radical Damage and its Control* (Rice-Evans, C. A., and Burdon, R. H., Eds.) pp 25−66, Elsevier, New York.
51. O'Neil, K. T., and DeGrado, W. F. (1990) *Trends Biochem. Sci. 15*, 59−64.
52. Meador, W. E., Means, A. R., and Quiocho, F. A. (1992) *Science 257*, 1251−1255.
53. Meador, W. E., Means, A. R., and Quiocho, F. A. (1993) *Science 262*, 1718−1721.
54. Ikura, M., Clore, G. M., Gronenborn, A. M., Zhu, G., Klee, C. B., and Bax, A. (1992) *Science 256*, 632−638.
55. Yin, D., Hühmer, A., Schöneich, Ch., and Squier, T. C. (1995) *Biophys. J. 68*, A165.
56. May, P. C., Osterburg, H. H., Mandel, R. J., Morgan, D. G., Randall, P. K., and Finch, C. E. (1987) *J. Neurosci. Res. 17*, 247−250.
57. May, P. C., Severson, J. A., Osterburg, H. H., and Finch, C. E. (1987) *Neurobiol. Aging 8*, 131−137.
58. Castro, M., Pedrosa, D., and Osuna, J. I. (1993) *Experientia 49*, 850−853.
59. Eckles, K. E., Dudek, E. M., Bickford, P. C., and Browning, M. D. (1997) *Neurobiol. Aging 18*, 213−217.
60. Mullany, P., Connolly, S., and Lynch, M. A. (1996) *Eur. J. Pharmacol. 309*, 311−315.
61. Clark, M. R., and Shohet, S. B. (1985) *Clin. Haematol. 14*, 223−257.
62. Clark, M. R. (1988) *Physiol. Rev. 68*, 503−554.
63. Moskovitz, J., Berlett, B. S., Poston, J. M., and Stadtman, E. R. (1997) *Proc. Natl. Acad. Sci. U.S.A. 94*, 9585−9589.
64. Gellman, S. H. (1991) *Biochemistry 30*, 6633−6636.
65. Williams, R. J. P. (1992) *Cell Calcium 13*, 355−362.
66. Bayley, P. M., Findlay, W. A., and Martin, S. R. (1996) *Protein Sci. 5*, 1215−1228.
67. Brown, S. E., Martin, S. R., and Bayley, P. M. (1997) *J. Biol. Chem. 272*, 3389−3397.
68. Chattopadhyaya, R., Meador, W. E., Means, A. R., and Quiocho, F. A. (1992) *J. Mol. Biol. 228*, 1177−1192.
69. Kraulis, P. J. (1991) *J. Appl. Crystallogr. 24*, 946−950.
70. Michaelis, M. L., Foster, C. T., and Jayawickreme, C. (1992) *Mech. Aging Dev. 62*, 291−306.

BI9803877